p53RDL1 regulates p53-dependent apoptosis

Chizu Tanikawa*†, Koichi Matsuda*†, Seisuke Fukuda*, Yusuke Nakamura* and Hirofumi Arakawa*‡§

*Human Genome Center, Institute of Medical Science, University of Tokyo, 4-6-1 Shirokanedai, Minato-ku, Tokyo 108-8639, Japan

†These authors equally contributed to this work.

‡e-mail: harakawa@gan2.res.ncc.go.jp

§Current address: Cancer Medicine and Biophysics Division, National Cancer Center Research Institute, 5-1-1 Tsukiji, Chuou-ku, Tokyo 104-0045, Japan

Published online: 24 February 2003; DOI: 10.1038/ncb943

Although a number of targets for p53 have been reported, the mechanism of p53-dependent apoptosis still remains to be elucidated. Here we report a new p53 target-gene, designated *p53RDL1* (p53-regulated receptor for death and life; also termed *UNC5B*). The *p53RDL1* gene product contains a cytoplasmic carboxy-terminal death domain that is highly homologous to rat Unc5H2, a dependence receptor involved in the regulation of apoptosis, as well as in axon guidance and migration of neural cells[1]. We found that p53RDL1 mediated p53-dependent apoptosis. Conversely, when p53RDL1 interacted with its ligand, Netrin-1, p53-dependent apoptosis was blocked. Therefore, p53RDL1 seems to be a previously un-recognized target of p53 that may define a new pathway for p53-dependent apoptosis. We suggest that p53 might regulate the survival of damaged cells by balancing the regulation of Netrin–p53RDL1 signalling, and cell death through cleavage of p53RDL1 for apoptosis.

The *p53* gene is mutated in more than half of all human cancers examined[2]. Endogenous expression of wild-type p53, where present, is activated transcriptionally and post-translationally by a variety of cellular stresses, such as heat shock, hypoxia, osmotic shock and DNA damage, which in turn can suppress tumour formation through transcriptional regulation of target genes that possess p53-binding site(s)[3]. Growth arrest, DNA repair and apoptosis are thought to constitute the core mechanisms of p53-dependent tumour suppression. To date, more than a dozen p53 target genes have been reported; $p21^{WAF1}$ is considered to be one of the most important, because it inhibits cyclin-dependent kinase and is essential for p53-dependent arrest of the cell cycle[4]. *p53R2* supplies nucleotides for DNA synthesis, allowing repair of damaged DNA[5,6]. Several mitochondrial proteins, including Bax[7], Noxa[8] and p53AIP1 (refs 9, 10) contribute to the release of cytochrome *c* from mitochondria. Other known apoptotic targets of p53 include Fas/ApoI (ref. 11) and Killer/DR5 (ref. 12), both of which are involved in the death-receptor-mediated apoptotic pathway. p53DINP1 (ref. 13) positively regulates p53-dependent apoptosis by enhancing phosphorylation of p53 on Ser 46. Given that at least 100 potential binding sites for p53 are probably present in the human genome[14], we predict that p53 might suppress tumour formation by transcriptionally regulating a large number of genes. To investigate the precise mechanism(s) of p53′s tumour-suppressive functions, it is essential to isolate and identify unknown target genes. Recently, we used cDNA-microarray technology to isolate additional p53 target-genes. This approach suggested that *p53RDL1*, a human counterpart of the rat *Unc5H2* gene, is yet another direct transcriptional target of p53.

We have used cDNA microarray analysis to isolate p53 target-genes, using mRNAs isolated from *p53*-mutant U373MG cells infected with either adenovirus-expressed (Ad)-p53 or Ad-LacZ, as described previously[15]. Of the 9216 human genes isolated, we selected one expressed sequence tag (EST; UniGene accession number Hs.183918) for further analysis because it was significantly upregulated (Fig. 1a, top). Northern blot analysis confirmed induction of its 4-kb and 7-kb transcripts in a time-dependent manner in U373MG cells infected with Ad-p53, but not with Ad-LacZ (Fig. 1a, bottom).

To isolate the full-length cDNA represented by this EST fragment, we constructed a cDNA library using poly(A)$^+$ RNA obtained from U373MG cells infected with Ad-p53. Next, we screened the library using a 300-bp non-coding fragment of the EST as a probe, resulting in the isolation of five independent clones. Sequence analysis of these clones revealed a transcript of 3935 nucleotides with an open reading frame encoding a peptide of 945 amino acids. A protein homology search using the BLAST program revealed significant homology (92% amino acid identity) between this product and a rat transmembrane receptor, Unc5H2 (see Supplementary Information, Fig. S1). Hence, we considered this gene to be a human counterpart of rat *Unc5H2* and designated it *p53RDL1* (also termed *UNC5B*). Interestingly, expression of *UNC5A* mRNA was also induced by p53 (data not shown). The SMART program predicted that the p53RDL1 protein would contain a transmembrane region in its middle portion and a death domain at the C-terminal end of the intracellular domain (Fig. 1b). Comparison of genomic (GenBank accession numbers AL359384, AL359832 and AC006187) and cDNA sequences defined the genomic structure shown in Fig. 1c. The *p53RDL1* gene consists of 17 exons that span a 90-kb genomic region on chromosome 10.

To determine whether *p53RDL1* is a direct target for p53, we searched for p53-binding sites (p53BSs) within its genomic sequence. Ten possible sites were identified in the promoter region and intron 1 that revealed an 80% or greater match to the previously proposed consensus p53-binding sequence[16]. To verify whether p53 could bind to these candidate p53BSs, we used chromatin immunoprecipitation (ChIP) assay to analyse cell lysates extracted from U373MG cells infected with an adenoviral vector designed to express wild-type p53. The 500-bp genomic fragment (p53BR1), including three possible sites, but not others, was specifically precipitated as a p53 protein–DNA complex with an anti-p53 antibody (Fig. 1c, d). The DNA fragment was also precipitated with an anti-p53 antibody using cell lysates extracted from HCT116 cells treated with the DNA-damaging agent, adriamycin, implying an interaction with endogenous p53 in response to the genotoxic stress (Fig. 1c). Thus, we evaluated the p53-dependent transcriptional activity of p53BR1 using a heterologous reporter assay. p53BR1, including three p53BSs (p53BS-A–C), was cloned upstream of the minimal SV40 promoter in pGL3. As a negative control, we also cloned another 500-bp fragment (p53BR2), including p53BS-D

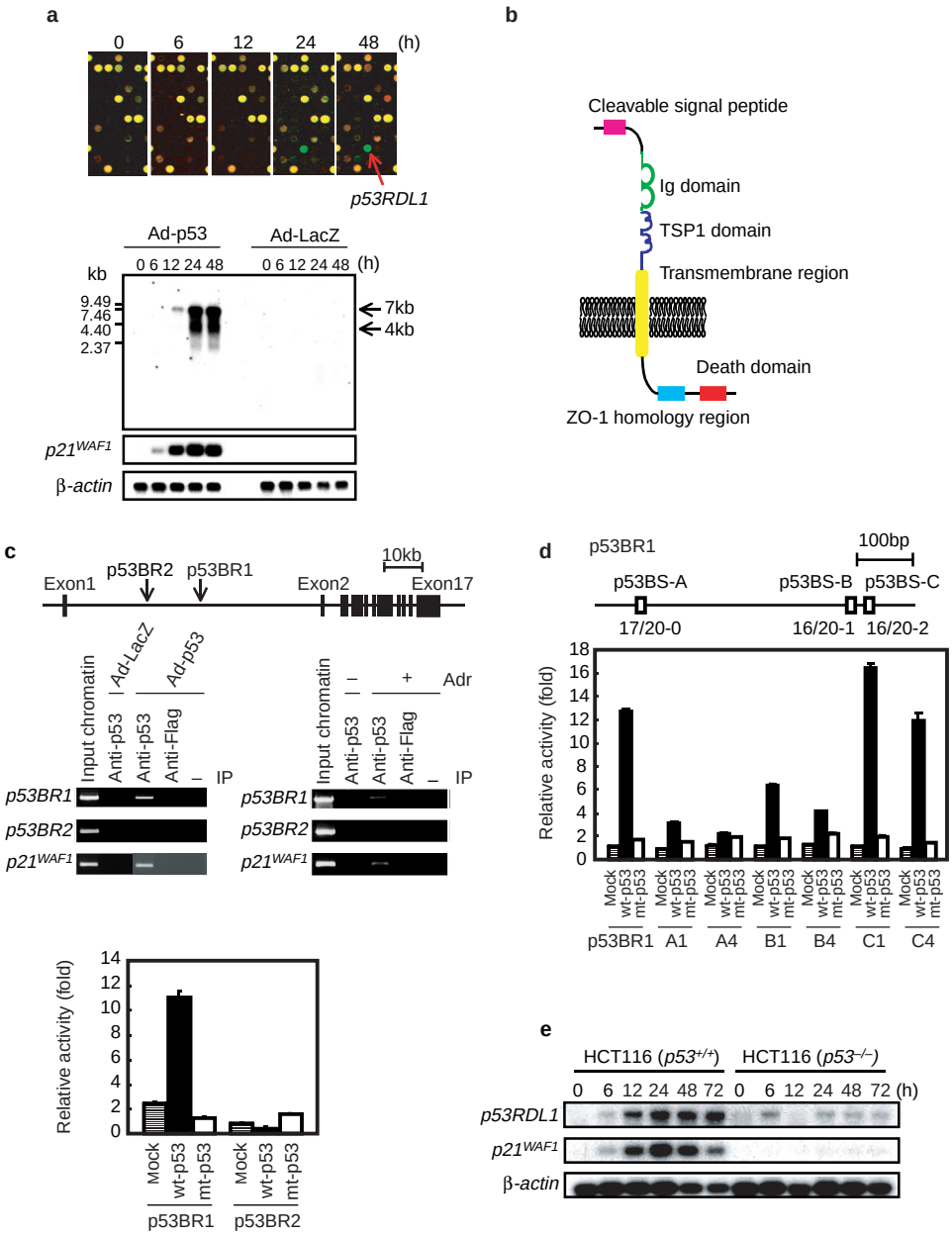

Figure 1 **Cloning of *p53RDL1* as a direct target of p53. a**, Induction of *p53RDL1* expression after infection with Ad-p53. Micro-array analysis (top). Green, expression induced by infection with Ad-p53; red, reduced expression by infection with Ad-p53; yellow, unchanged expression; black, no detectable expression. Changes in relative expression are presented in graduated colour patterns at the indicated times after infection with Ad-p53 or Ad-LacZ. Northern blot analysis (bottom) of *p53RDL1* mRNA expression in U373MG cells at the indicated times after infection with Ad-p53 or Ad-LacZ is shown. *p21*^{WAF1} and *β-actin* probes were used as positive and loading controls, respectively. **b**, Domain structure of p53RDL1 protein. **c**, Identification of p53BR in the genomic DNA of *p53RDL1*. Black boxes indicate the locations and relative sizes of 17 exons; an arrow indicates the potential p53-binding regions (p53BR1, p53BR2; top). ChIP assay was performed on genomic fragments, p53BR1 and p53BR2 (middle). Left panel shows Ad-p53-infected (lanes 1, 3–5) or Ad-LacZ-infected (lane 2) U373MG cells. Right panel shows adriamycin (Adr)-treated (lanes 1, 3–5) or untreated (lane 2) MCF7 cells. Samples were immunoprecipitated with an anti-p53 antibody (lane 2, 3) before PCR amplification. Input chromatin represents a portion of the sonicated chromatin before immunoprecipitation (lane 1). Immunoprecipitates with an anti-Flag antibody (lane 4) or in the absence of antibody (lanes 5) were used as negative controls. Luciferase assay (bottom). Luciferase activity is indicated relative to the activity of pGL3-promoter vector without p53BSs. **d**, The functional p53-binding sequences of *p53RDL1*. Genomic structure of p53BR1 (top). White boxes indicate the locations of p53BSs (A–C). The figures under white boxes indicated the number of nucleotides that are identical to the p53 consensus sequence[16] and spacer sequences. A luciferase assay of p53BSs is shown (bottom). **e**, Endogenous p53-dependent induction of *p53RDL1* transcription in *p53*$^{+/+}$ or *p53*$^{-/-}$ HCT116 cells after DNA damage by treatment with 1 μg ml^{-1} adriamycin. *β-actin* expression was used as a loading control.

(Fig. 1c), which was not precipitated in the p53 ChIP assay. The activity of p53BR1 fused to the luciferase gene was strongly enhanced by cotransfection with wild-type p53, but not by cotransfection with mutant p53, whereas the activity of p53BR2–luciferase was not enhanced by either of the plasmids (Fig. 1c). Moreover, the plasmids containing a point mutation(s) of p53BS-A and p53BS-B (A1,

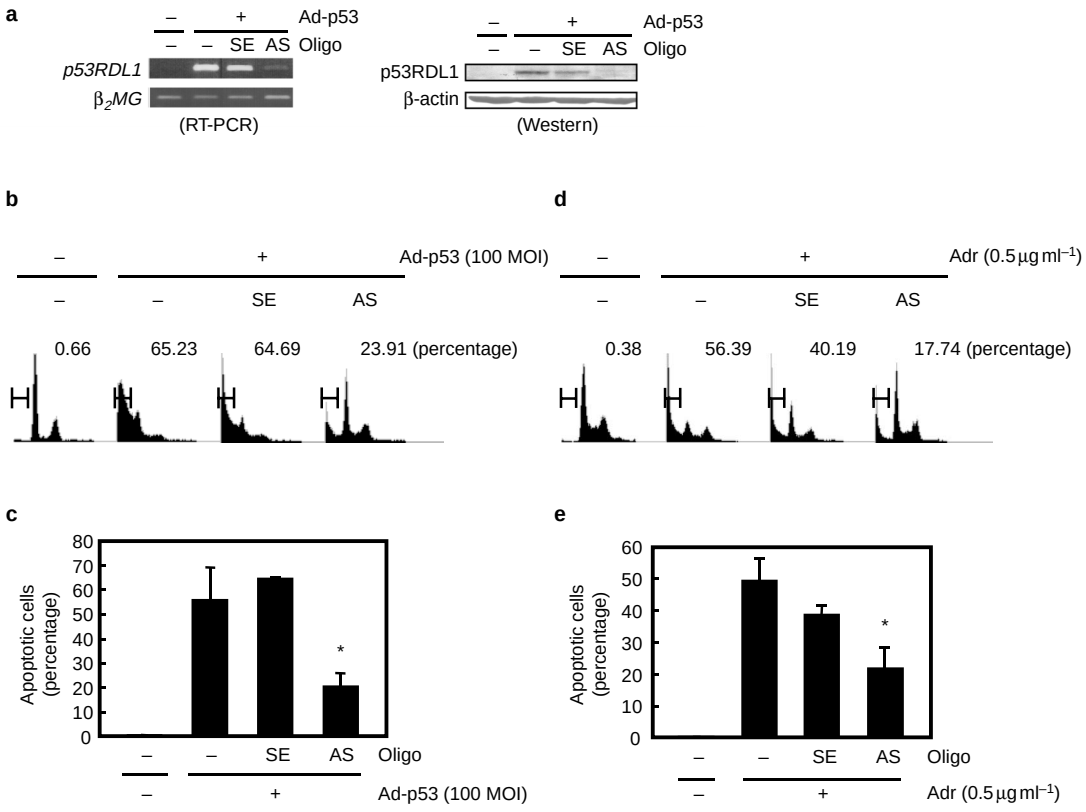

Figure 2 **p53RDL1 as a mediator of p53-dependent apoptosis. a**, Inhibition of *p53RDL1* expression with antisense oligonucleotides. Antisense (AS) or sense (SE) oligonucleotides (1 μM) were transfected into U373MG cells before infection with Ad-p53. *p53RDL1* expression was examined by RT-PCR (left) and western blotting (right) 48 h after infection. β_2-microglobulin (β_2MG) and β-actin were used as loading controls. **b**, Inhibition of Ad-p53-induced apoptosis by AS oligonucleotide. Proportions of apoptotic cells were indicated as a percentage of the sub-G1 fraction in FACS analysis. **c**, A graphic representation of **b**. **d**, Inhibition of DNA damage-induced apoptosis by AS oligonucleotide. Apoptosis was assessed as in **b**. **e**, A graphic representation of **d**. Experiments were repeated three times and averaged scores are shown with error bars in **c** and **e**. $^*P < 0.01$ (**c**) or $^*P < 0.05$ (**e**), compared with s.e.m.; Student-Newman-Keuls *t* test. The representative data of three independent experiments are shown in **b** and **d**.

A4, B1 and B4) showed a significant decrease of $p53^{WT}$-dependent transcriptional activity (Fig. 1d), suggesting that both p53BS-A and p53BS-B are the functional p53-binding sequence. Taken together, these results clearly indicate that *p53RDL1* is a genuine target for p53. Consistently, expression of *p53RDL1* mRNA was induced in MCF7 cancer cells ($p53^{+/+}$), but not in H1299 cancer cells ($p53^{-/-}$), by treatment with adriamycin or γ- or ultraviolet (UV) irradiation (see Supplementary Information, Fig. S2a). This suggests that transcription of *p53RDL1* can be activated by various cellular stresses in a p53-dependent manner. Moreover, the result was also reproduced in isogenic $p53^{+/+}$ and $p53^{-/-}$ HCT116 colon cancer cell lines (Fig. 1e).

Ectopically expressed haemagglutinin (HA)-tagged p53RDL1 (HA–p53RDL1) localized to the plasma membrane (see Supplementary Information, Fig. S2b, c). After infection with Ad-p53, expression of endogenous p53RDL1 protein (relative molecular mass (M_r) 110,000) increased until 24 h, but decreased thereafter in concert with the appearance of a smaller band (60K), described below as the 'cleaved band' (see Supplementary Information, Fig. S2d). Immunostaining of endogenous p53RDL1 proteins with an anti-p53RDL1 antibody confirmed the localization of p53RDL1 to the plasma membrane (see Supplementary Information, Fig. S2e).

To investigate a potential role of p53RDL1 in p53-dependent apoptosis, we inhibited expression of p53RDL1 in U373MG glioblastoma cells by preparing four different antisense oligonucleotides (AS1–AS4) and the corresponding sense oligonucleotides (SE1–SE4), according to the sequence of *p53RDL1* cDNA (see Methods). Treatment with AS1 and AS2 (data not shown) or AS3 (Fig. 2a) clearly suppressed expression of *p53RDL1* mRNA and protein. Inhibition of *p53RDL1* expression by pre-treatment with AS1, AS2 (data not shown) or AS3 (Fig. 2b, c) induced a marked block in Ad-p53-induced apoptosis. Furthermore, inhibition of *p53RDL1* expression by AS3 partially blocked apoptosis induced by DNA damage after exposure to adriamycin (Fig. 2d, e), which is partially p53-dependent. These results suggest that p53RDL1 contributes to p53-dependent apoptosis.

We constructed an adenovirus vector containing wild-type or mutant (D412N) p53RDL1 cDNA, which was previously described as an essential cleavage site for caspase-3 during rat Unc5H2-induced apoptosis[1], and infected it into several cancer cell lines. Both Ad-$p53RDL1^{WT}$ and Ad-$p53RDL1^{D412N}$ were expressed and localized to the plasma membrane of infected U373MG cells (Fig. 3a). Induction and overexpression of $p53RDL1^{WT}$, but not $p53RDL1^{D412N}$, induced apoptosis and activated caspase-3 in U373MG cells (Fig. 3b, c). Furthermore, a specific caspase-3 inhibitor significantly blocked induction of apoptosis by $p53RDL1^{WT}$ (Fig. 3d). Similar results were obtained with A172 (glioblastoma), U87MG (glioblastoma), DBTRG-05MG (glioblastoma), SW480 (colon cancer), Lovo (colon cancer), MCF7 (breast-cancer) (Fig. 3e) or H1299 (lung cancer) cells (data not shown). The extent of $p53RDL1^{WT}$-induced apoptosis in the four glioblastoma cell lines examined (U373MG, A172, U87MG and DBTRG-05MG) was higher than in the other types of cancer cell (Lovo,

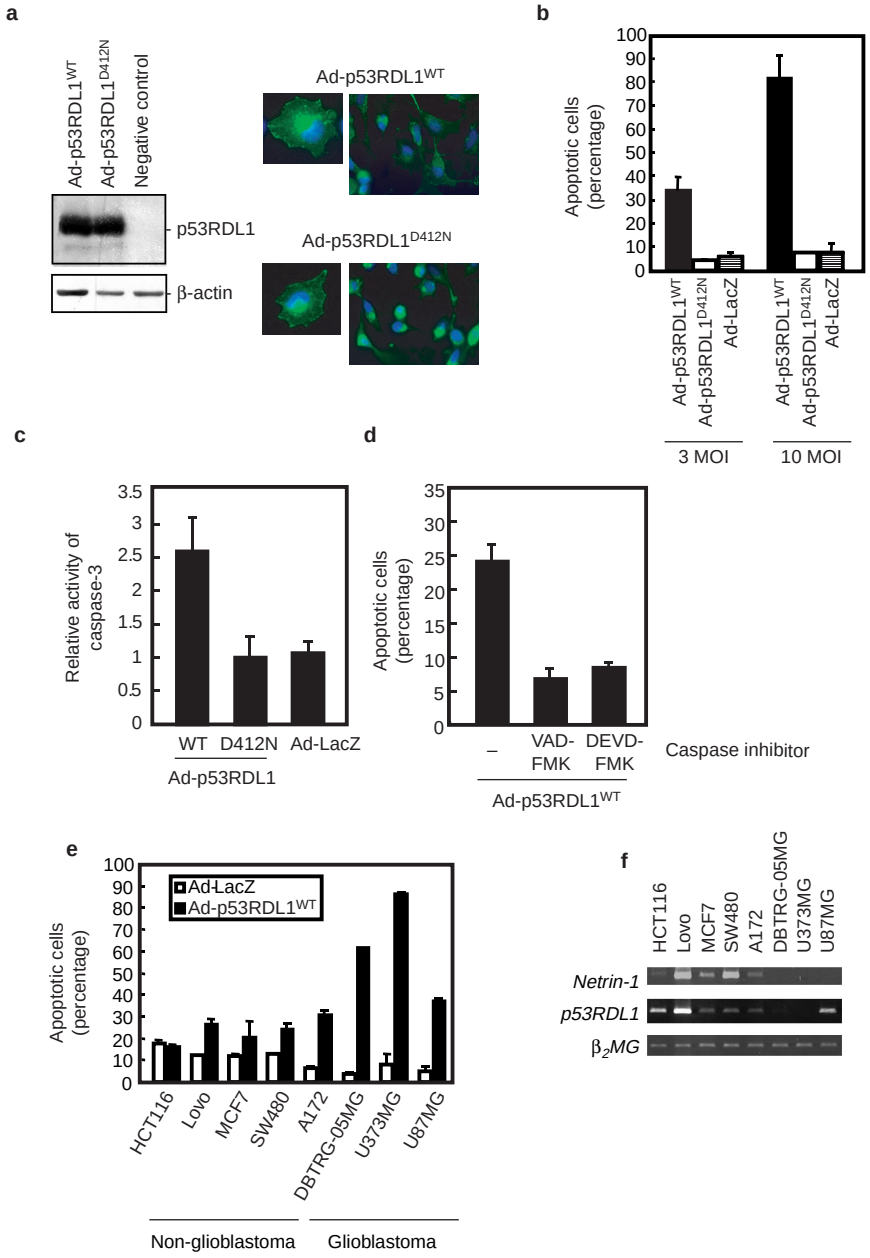

Figure 3 Induction of apoptosis by Ad-p53RDL1 in glioblastoma cell lines. a, Expression of Ad-p53RDL1^{WT} or Ad-p53RDL1^{D412N} in U373MG cells was examined by western blotting and immunofluorescence microscopy with rabbit polyclonal anti-p53RDL1 antibody. The negative control shows U373MG cells not infected with adenovirus. b, Induction of apoptosis by infection with Ad-p53RDL1^{WT}. c, Activation of caspase-3 by infection with Ad-p53RDL1^{WT}. d, Inhibition of Ad-p53RDL1^{WT}-induced apoptosis in U373MG cells with specific caspase-3 inhibitors. e, Induction of apoptosis by Ad-p53RDL1^{WT} in diverse cancer cell lines. f, Netrin-1 expression in diverse cancer cell lines. Netrin-1 and p53RDL1 expression was examined by RT-PCR. U373MG cells (a–e) and other indicated cells (e) were infected with Ad-p53RDL1^{WT}, Ad-p53RDL1^{D412N} or Ad-LacZ at 3 MOI (b) or 10 MOI (a–e). Apoptotic cells were evaluated by FACS. The experiments were repeated three times, and averaged scores are shown with error bars.

SW480, MCF7 and HCT116). Interestingly, the expression levels of Netrin-1 in these glioblastoma cell lines were much lower than those in non-glioblastoma cell lines (Fig. 3f). This may imply a potential application of adenovirus-mediated *p53RDL1* gene therapy for patients with glioblastoma. The results of our experiments, combined with others, strongly suggest that cleavage of p53RDL1 at Asp 412 is crucial for p53RDL1-induced apoptosis, and possibly represents a major pathway for p53-dependent apoptosis.

As an uncleaved form of rat Unc5H2 was shown to have no apoptosis-inducing activity when bound to Netrin-1 (ref. 1), we speculated that the Netrin–p53RDL1 signalling pathway might affect regulation of p53-dependent apoptosis. An *in vitro* pull-down assay clearly demonstrated that glutathione *S*-transferase (GST)–Netrin-1, but not GST alone, interacted with p53RDL1 protein produced in COS7 (Fig. 4a) or U373MG cells (data not shown). This indicates that GST–Netrin-1 can bind to ectopically expressed p53RDL1 in our system. In addition, we examined whether GST–Netrin-1 is biologically active with regard to Netrin-

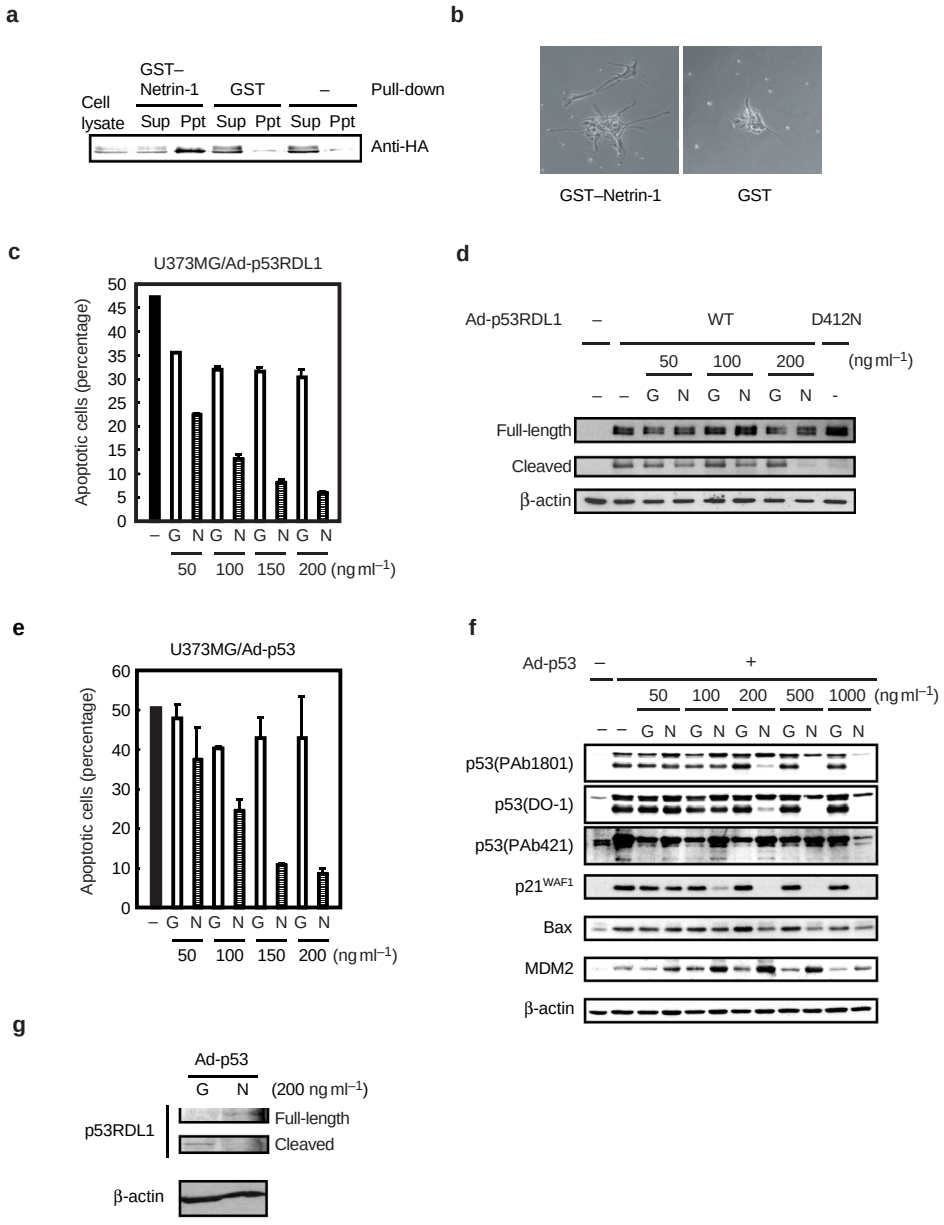

Figure 4 **Netrin-1 inhibits p53-induced apoptosis. a**, GST pull-down assay. HA-tagged full-length p53RDL1 protein was bound only to GST–Netrin-1. Sup: supernatant; Ppt: precipitates. **b**, Induction of axon outgrowth by GST–Netrin-1 in NHNP cells. NHNP cells were incubated with 200 ng ml^{-1} GST–Netrin-1 or GST alone for 48 h. **c**, Inhibition of p53RDL1-induced apoptosis in U373MG cells after treatment with Netrin-1. Cells were incubated with either GST–Netrin-1 (G) or Netrin-1 (N). **d**, Western blot showing that cleavage of exogenous p53RDL1 protein is inhibited by Netrin-1. **e**, Inhibition of p53-induced apoptosis in U373MG cells after treatment with Netrin-1. **f**, Western blots showing altered expression of p53 target genes after treatment with Netrin-1. **g**, Western blot showing that cleavage of endogenous p53RDL1 protein is inhibited by treatment with Netrin-1. Experiments were repeated independently three times. The averages of apoptotic cells are shown with error bars indicating one standard deviation (**c**, **e**).

mediated outgrowth of axons in normal human neural progenitor (NHNP) cells. Addition of GST–Netrin-1, but not GST alone, induced axonal outgrowth (Fig. 4b). Next, GST–Netrin-1 was used to investigate whether Netrin-1 could block p53RDL1-induced apoptosis. Infection with Ad-p53RDL1 elevated p53RDL1 protein levels in U373MG cells, resulting in a marked induction of apoptosis (Fig. 4c, d). However, addition of physiological concentrations of GST–Netrin-1 (0.05–0.2 μg ml^{-1}) to the culture medium suppressed Ad-p53RDL1-induced apoptosis of U373MG cells, as well as cleavage of p53RDL1 protein (Fig. 4c, d), suggesting that the interaction of Netrin-1 with p53RDL1 in fact had a positive effect on cell survival. Thus, we examined a possible role of Netrin-1 in p53-induced apoptosis. As expected, GST–Netrin-1 blocked Ad-p53-induced apoptosis in a dose-dependent manner (Fig. 4e). To clarify the mechanism of this phenomenon, we further examined expression of p53 using the same lysates. Expression levels of full-length p53 were unaffected by low concentrations of Netrin-1 (50–200 ng ml^{-1}), but were significantly reduced by high concentrations (500–1000 ng ml^{-1}). However, expression of 'small' p53 (the 43K cleaved form detected by anti-p53 antibodies against the amino terminus of p53, such as Pab1801 and DO-1) was affected, even at the lower concentration (200 ng ml^{-1}) of Netrin-1. Small

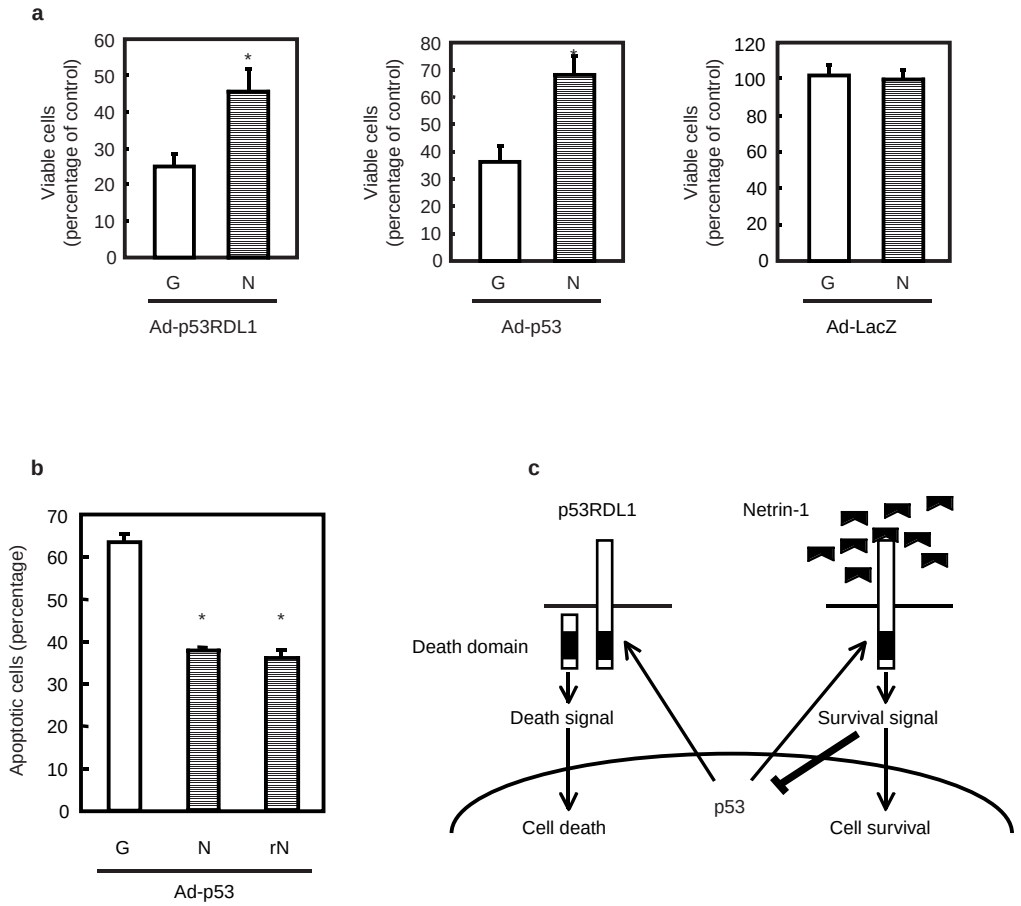

Figure 5 **Netrin-1 inhibits p53-induced neuronal cell death. a**, Effects of Netrin-1 on Ad-p53RDL1- or Ad-p53-induced apoptosis in NHNP cells. NHNP cells were infected with Ad-p53RDL1, Ad-p53 or Ad-LacZ at 10 MOI before incubation with 200 ng ml^{-1} GST–Netrin-1 (N) or GST (G). After 48 h (Ad-p53, Ad-LacZ) or 72 h (Ad-p53RDL1), cell viability was estimated in triplicate by MTT assay. Results are given as percentage against control NHNP cells (incubated without viral infection). **b**, Effects of Netrin-1 on Ad-p53-induced apoptosis in PC-12 cells. PC-12 cells were seeded in the presence of 100 ng ml^{-1} nerve growth factor (NGF) 48 h before infection. Neuronal differentiation was observed in more than 80% of cells. Cells were infected with Ad-p53 and incubated with 200 ng ml^{-1} GST–Netrin-1 (N), GST–rat Netrin-1 (rN) or GST alone (G). Proportions of apoptotic cells were determined by FACS analysis 48 h after infection. The experiments were repeated independently three times and the averages of apoptotic cells are shown with error bars indicating one standard deviation (**a**, **b**). *P < 0.05 (**a**) or *P<0.01 (**b**), compared with GST; Student-Newman-Keuls t test. **c**, A hypothetical model for regulation of cell death and survival through the p53RDL1–Netrin-1 interaction in the putative p53-dependent apoptotic pathway.

p53 was not detected by the anti-p53 antibody, raised against the C terminus of p53 (PAb421), suggesting that it probably lacks this region. We also examined the expression of several p53 targets by western blotting. Interestingly, expression of *p21*^{WAF1} and *BAX* were decreased at the lower (50 ng ml^{-1}) concentration of Netrin-1. Conversely, expression of *MDM2* was enhanced at this concentration. Finally, consistent with the data shown in Fig. 4d, GST–Netrin-1 also suppressed Ad-p53-induced cleavage of endogenous p53RDL1 protein (Fig. 4g). Although the details of the mechanism remain to be elucidated, these results indicate that the Netrin–p53RDL1 signalling pathway could influence p53 activity post-translationally, resulting in impairment of p53-dependent apoptosis.

To further validate our hypothesis in biologically relevant cell types, we performed adenovirus-mediated *p53RDL1* and/or *p53* expression assays in primary neuronal cells derived from NHNP cells. Adenovirus-mediated expression of *p53RDL1* or *p53* induced cell death in 75% or 65% of primary neuronal cells, suggesting that p53RDL1 and p53 are important for apoptosis of primary neuronal cells. In contrast, control *LacZ*-infected cells were unaffected. We confirmed that cell death was caused by apoptosis using the TUNEL assay coupled with the immunofluorescence staining method (data not shown). Furthermore, addition of 200 ng ml^{-1} Netrin-1 to this system significantly inhibited p53RDL1- or p53-induced apoptosis of primary neuronal cells from 75% to 55% and 65% to 30%, respectively (Fig. 5a). These results are consistent with our analysis of U373MG cells (Fig. 4). Moreover, similar results were obtained in experiments with neuronal cells differentiated from PC-12 cells (Fig. 5b). In these systems, adenovirus was efficiently infected into NHNP cells or PC-12 cells, as shown by β-galactosidase staining (see Supplementary Information, Fig. S3). Taken together, these results clearly suggest that activation of p53 can induce neuronal apoptosis and that the Netrin–p53RDL1 pathway, triggered by p53, might positively and negatively regulate neuronal apoptosis.

The interplay of Netrins and their respective receptors is critical for determining the direction and extent of cell migration and axonal outgrowth during neuronal development[17]. Although a number of studies have demonstrated the importance of the Netrin–Netrin receptor pathway with regard to chemo-attractant

and chemorepellent effects on development of the nervous system[17,18,19], recent studies have provided clear evidence that the Netrin-1 receptors, DCC (deleted in colorectal cancer) and UNC5H, are pivotal in the regulation of apoptosis when expressed in the absence of Netrin-1 (refs 20, 21). It seems that a pathway involving Netrin-1 and DCC, or Netrin-1 and UNC5H, might regulate two diverse functions; that is, cell survival and cell death, determined by the presence or absence of Netrin-1. Interestingly, a new p53 target-gene *p53RDL1* encodes the human homologue of rat Unc5H2 (also designated UNC5B). In this study, we demonstrate that p53RDL1 mediated p53-dependent apoptosis. Moreover, the interaction of Netrin-1 with p53RDL1 clearly blocked p53-dependent apoptosis. Surprisingly, signalling of the Netrin1–p53RDL1 pathway did not affect the levels of p53 protein at the low concentration of Netrin-1, whereas expression of *p21*, *BAX* and *MDM2* were altered at concentrations as low as 50 ng ml^{-1}. The role of Netrin-1 in the p53-regulated human p53RDL1 pathway remains to be fully elucidated, but these results imply that p53 might be a determinant for balance between cell survival and apoptosis. We speculate that induction of *p53RDL1* expression by p53 may be necessary for both cell survival and cell death (Fig. 5c). Hence, our finding that p53 directly regulates p53RDL1-dependent apoptotic activity seems to have defined a previously unrecognized pathway for p53-dependent apoptosis. The discovery of this pathway could provide new insights into the complex physiological function of p53. □

Methods

Cell culture and transfections

Human cancer cell lines U373MG (glioblastoma), MCF7 (breast carcinoma), H1299 (lung carcinoma), HCT116 (colorectal adenocarcinoma), Lovo (colorectal adenocarcinoma), SW480 (colorectal adenocarcinoma), A172 (glioblastoma), DBTRG-05MG (glioblastoma), U87MG (glioblastoma), COS-7 (monkey, kidney) and PC-12 (rat pheochromocytoma) were purchased from American Type Culture Collection. HCT116 ($p53^{+/+}$ and $p53^{-/-}$) cell lines were gifts from B. Vogelstein (Johns Hopkins University, Baltimore, MD). NHNP cells were purchased from Cambrex Co. (East Rutherford, NJ). All cells were cultured under conditions recommended by their respective depositors.

For transfection, cells were seeded at 2×10^5 cells per six-well plate. After 24 h, cells were transfected with 1 μg of plasmid mixtures pre-incubated for 15 min with 6 μl of Fugene6 transfection reagent (Roche, Basel, Switzerland).

Plasmids

The entire coding sequence of *p53RDL1* cDNA was amplified by PCR using KOD-Plus DNA polymerase (Toyobo, Osaka, Japan), and inserted into the *Eco*RI and *Xho*I sites of pcDNA3.1$^+$ (Invitrogen, San Diego, CA), which carries a cytomegalovirus (CMV) promoter and a gene conferring neomycin resistance (pcDNA-p53RDL1, pcDNA-IC-p53RDL1). An HA epitope tag was placed at the C terminus (pcDNA-HA-p53RDL1) of the expression vector. Constructs were confirmed by sequencing. Primer sequences were forward, 5′-AAAGAATTCCCGCGGGAGCATGGGGGCCC-3′; reverse, 5′-TTTCTCGAGTCAGCAGTCCCCGTCGGTGG-3′; and HA-reverse, 5′-TTTCTCGAGTCAAGCGTAGTCTGGGACGTCGTATGGGTAGCAGTCCCCGTCGGTGG-3′.

Constructs encoding p53RDL1 with codon 412 (Asp) mutated to Asn were derived from pcDNA-p53RDL1 by site-directed mutagenesis (pcDNA- p53RDL1^{D412N}). In brief, the QuikChange site-directed mutagenesis kit (Stratagene, La Jolla, CA) was applied according to the manufacturer's instructions, using oligonucleotides 5′-GACACAGACATCACTAACTCATCTGCTGCCC-3′ and 5′-GGGCAGCAGATGAGTTAGTGATGTCTGTGTC-3′. Changes were confirmed by DNA sequence analysis.

Construction of recombinant adenovirus and infection of cells

Replication-deficient recombinant viruses Ad-p53RDL1^{WT}, Ad-p53RDL1^{D412N}, Ad-p53 and Ad-LacZ, encoding p53RDL1^{WT}, p53RDL1^{D412N}, p53 and LacZ, respectively, were generated and purified, as described previously[9]. U373MG cells were infected with viral solutions at an indicated multiplicity of infection (MOI) and incubated at 37 °C until the time of harvest.

ChIP assay

ChIP assay was performed using the acetyl-histone H3 ChIP Assay Kit (Upstate Biotechnology, Waltham, MA), as recommended by the manufacturer, except that antibodies against p53 (Ab-12) and the Flag tag peptide (M2) were used in this study. 2×10^6 U373MG cells or MCF7 cells were plated onto a 10-cm dish and infected with Ad-p53 or Ad-LacZ, or treated with adriamycin (Adr). After 40 h, genomic DNA and protein were cross-linked by addition of formaldehyde (1% final concentration) directly to culture medium and incubated for 10 min at 37 °C. Cells were lysed in 200 μl SDS lysis buffer (1% SDS, 10 mM EDTA and 50 mM Tris-HCl at pH 8.1) with protease inhibitor cocktail tablets (Roche) and sonicated to generate 300–1000-bp DNA fragments. After centrifugation, the cleared supernatant was diluted tenfold with ChIP dilution buffer and precleared by incubation with protein A–Sepharose beads at 4 °C for 30 min with agitation. The precleared supernatant was incubated with the specific antibody at 4 °C for 16 h with rotation before incubation with protein A–Sepharose beads at 4 °C for 1 h with rotation. Immune complexes were precipitated, washed and eluted as recommended. DNA–protein cross-links were reversed by heating to 65 °C for 5 h. DNA was phenol-extracted, ethanol-precipitated and resuspended in 50 μl of Tris-EDTA. We used 1 μl of each sample as a template for PCR amplification. PCR amplifications of *p53RDL1* intron 1, containing the consensus p53-binding sites, were performed on immunoprecipitated chromatin using the specific primers, 5′-AGCCGTCCAGGACCTGTCTG-3′ (p53BR1, forward) and 5′-CTGACTGCAACGTCTGGGAG-3′ (p53BR1, reverse), or 5′-GCCGCCAGGAGATTAGAAAC-3′ (p53BR2, forward) and 5′-AAGAATGAAGCCTCATCTCC-3′ (p53BR2, reverse), or 5′-ACCTTTCACCATTCCCCTAC-3′ ($p21^{WAF1}$, forward) and 5′-GCCCAAGGACAAAATAGCCA-3′ ($p21^{WAF1}$, reverse), respectively. To ensure that PCR was performed in linear range, template DNA was amplified for a maximum of 30 cycles.

Gene reporter assays

A DNA fragment, including potential p53-binding sites of p53RDL1, was amplified by PCR, digested with *Mlu*I and *Xho*I and cloned into the pGL3-promoter vector (Promega, Madison, WI). Primer sequences were, for *p53RDL1*: p53BR1-forward, 5′-AAAACGCGTAGCCGTCCAGGACCTGTCTG-3′ and p53BR1-reverse, 5′-TTTCTCGAGCTGACTGCAACGTCTGGGAG-3′ or p53BR2-forward, 5′-AAAACGCGTGCCGCCAGGAGATTAGAAAC-3′ and p53BR2-reverse, 5′-TTTCTCGAGAAGAATGAAGCCTCATCTCC-3′.

To make A1, B1 and C1, a point mutation 'T' was inserted into the site of the seventh nucleotide 'G' of each BS using the QuickChange site-directed mutagenesis kit (Stratagene). To make A4, B4 and C4, a point mutation 'T' was inserted into the site of the fourth nucleotide 'C', the seventh nucleotide 'G', the fourteenth nucleotide 'C' and the seventeenth nucleotide 'G' of the consensus p53-BS.

U373MG cells were plated in six-well culture plates (1.5×10^5 cells per well) 24 h before cotransfection of 250 ng of reporter plasmid and either 250 ng of wild-type or mutant p53 expression vector in combination with 70 ng of pRL-CMV vector. At 36 h after transfection, cells were rinsed with PBS and lysed in 500 μl of a passive lysis buffer (Promega).

Lysates were used directly in the Dual Luciferase assay system (Promega), which depends on sequential measurements of firefly and Renilla luciferase activities in specific substrates (beetle luciferin and coelenterazine, respectively). Quantification of luciferase activities and calculations of relative ratios were performed manually with a luminometer.

DNA-damaging treatments

Cells were seeded 24 h before treatment and were 60–70% confluent at the time of treatment. To examine the expression of *p53RDL1* in response to genotoxic stresses, MCF7, H1299 and HCT116 ($p53^{+/+}$ and $p53^{-/-}$) cells were continuously treated with 1 μg ml^{-1} adriamycin for 2 h, UV-irradiated at 10 J m^{-2} using a UV cross-linker (Stratagene) or γ-irradiated at 50 Gy using a ^{60}Co source. For FACS analysis, MCF7 cells were continuously treated with 0.5 μg ml^{-1} adriamycin for 18 h. For ChIP analysis, MCF7 cells were continuously treated with 1 μg ml^{-1}adriamycin for 2 h.

Antibodies

Rabbits were immunized with the recombinant C-terminal intracellular domain of p53RDL1. Antibodies were subsequently purified on antigen affinity columns. Rat monoclonal anti-HA antibody (clone 3F10) was purchased from Roche. Mouse monoclonal anti-β-actin (clone AC15) was purchased from Sigma (St Louis, MO). Mouse monoclonal anti-p53 Ab-12 (clone DO-7), Ab-6 (clone DO-1), Ab-1 (clone PAb421), Ab-2 (clone PAb1801) and mouse monoclonal anti-$p21^{WAF1}$ (clone EA10) were purchased from Calbiochem (San Diego, CA). Mouse monoclonal anti-Flag (clone M2) was purchased from Sigma. Rabbit polyclonal anti-Mdm2 (C-18) and anti-Bax (N-20) were purchased from Santa Cruz Biotechnology (Santa Cruz, CA).

Western blot analysis

For preparation of whole-cell lysates, adherent and detached cells were collected and lysed in chilled RIPA buffer (50 mM Tris-HCl at pH 8.0, 150 mM sodium chloride, 0.1% SDS, 0.5% DOC, 1% NP-40 and 1 mM phenyl methylsulphonyl fluoride (PMSF)) for 30 min on ice. Homogenates were centrifuged for 15 min in a microcentrifuge at 4 °C and the supernatants were collected and boiled in SDS sample buffer. Each sample (10 μg) was loaded onto a 12% SDS–polyacrylamide gel electrophoresis (PAGE) gel and blotted onto a nitrocellulose membrane (Amersham, Buckinghamshire, UK). Protein bands on western blots were visualized by chemiluminescent detection (ECL; Amersham). For detection of endogenous hUNV5H2 protein, collected cells were lysed directly in 5× SDS sample buffer (125 mM Tris-HCl at pH 6.8, 4% SDS, 20% glycerol, 10% β-mercaptoethanol and 0.4 mg ml^{-1} Bromophenol Blue).

Immunocytochemistry

Adherent cells were fixed with 4% paraformaldehyde in PBS and permeabilized with 0.2% Triton X-100 in PBS for 5 min at room temperature. The cells were then covered with blocking solution (3% BSA/PBS containing 0.2% Triton X-100) for 30 min at room temperature and incubated with rat anti-HA antibody (diluted 1:1000) or rabbit anti-p53RDL1 antibody (2 μg ml^{-1}) in blocking solution for 60 min at room temperature. Primary antibodies were stained with goat anti-rat or anti-rabbit secondary antibodies conjugated to fluorescein isothiocyanate (FITC; each diluted 1:1000) for 1 h at room temperature, stained with DAPI and visualized with an ECLIPSE E600 microscope (Nikon, Tokyo, Japan).

Antisense oligonucleotides

To inhibit expression of endogenous p53RDL1, we prepared HPLC-purified anti-sense oligonucleotides (AS1: GCCCCCATGCTCCCGC; AS2: CGCTCCGGGCCCCCAT; AS3: GCTCCGCTCCGGGCCC; AS4: TCCTACCTGCTTGGCT) and, as a control, sense oligonucleotides (SE1: GCGGGAGCATGGGGGC; SE2: ATGGGGGCCCGGAGCG; SE3: GGGCCCGGAGCGGAGC; SE4: AGCCAAGCAGGTAGGA) according to the sequence of the *p53RDL1* gene. Antisense oligonucleotides (1 μM) were transfected with Lipofectin reagent (Invitrogen) for 4 h. Cells were then infected with either Ad-p53 or Ad-LacZ, or incubated with 0.5 μg ml^{-1} adriamycin for 18 h. Apoptotic cells were analysed by FACS.

Semi-quantitative RT-PCR analysis

The RT-PCR exponential phase was determined on 15–30 cycles to allow semi-quantitative comparisons among cDNAs developed from identical reactions. Each PCR regime involved a 2-min initial denaturation step at 94 °C, followed by 25 cycles (for *p53RDL1*), 30 cycles (for *Netrin-1*), or 19 cycles (for β_2*MG*) at 94 °C for 30 s, 55 °C for 30 s and 72 °C for 30 s on a Gene Amp PCR system 9700 (Applied Biosystems, Foster City, CA). Primer sequences were, for *p53RDL1*: forward, 5′-TGGCTCCCTGGACACTCTC-3′ and

reverse, 5′-CCACCAGCATCTCACTCTTG-3′; for *Netrin-1*: forward, 5′-CTGAAGACTGCGATTCCTAC-3′ and reverse, 5′-TCTTCTCACGCTGCTGGAAC-3′; for β_2*MG*: forward, 5′-CACCCCCACTGAAAAAGATGA-3′ and reverse, 5′-TACCTGTGGAGCAACCTGC-3′.

Detection of apoptosis

For FACS analysis, adherent and detached cells were combined and fixed with 70% ethanol at 4 °C. After two rinses with PBS, cells were incubated for 30 min with 1 ml of PBS containing 1 mg of boiled RNase at 37 °C. Cells were then stained in 1 ml of PBS containing 50 μg of propidium iodide. The percentages of sub-G1 nuclei in the population were determined from at least 2×10^4 cells in a flow cytometer (FACScalibur; Becton Dickinson, San Diego, CA). Caspase inhibitors, VAD-FMK and YVAD-FMK (MBL, Vagoya, Japan) were added at 20 μM after infection.

Caspase activity assay

Activities of caspase-3 were monitored using a caspase-3 assay kit that utilizes the DEVD-pNA substrate, according to the manufacturer's instructions (MBL). In this system, caspase activation is presented as the ratio between the caspase activity of the sample and that measured in untreated cells.

GST pull-down assays

GST–Netrin-1 and GST–rat-Netrin-1 were created by cloning the coding sequences, excluding the sequences encoding the N-terminal signal peptides, into pGEX5X-1 (Amersham). Proteins were expressed in *Escherichia coli* and purified on glutathione–Sepharose beads (Amersham) by standard methods. After transfection with a plasmid encoding HA-tagged full-length *p53RDL1*, COS-7 cells were washed in PBS and cell lysates were prepared by adding 1.5 ml of lysis buffer (20 mM Tris-HCl at pH 8.0, 200 mM sodium chloride, 1 mM EDTA at pH 8.0 and 0.5% NP-40) supplemented with 25 μg ml^{-1} PMSF. Lysates were precleared by incubation with 50 μl of 50% glutathione–Sepharose beads and 25 μg GST at 4 °C for 2 h. Next, 500 μl of precleared cell lysates were incubated with 50 μl of 50% glutathione–Sepharose beads and 10 μg of GST–Netrin-1 or GST alone at 4 °C for 2 h. The beads were washed three times in 1 ml of ice-cold lysis buffer and immune complexes were released from the beads by boiling in sample buffer for 5 min. After electrophoresis on 10% SDS–PAGE gels, immunoprecipitation products were analysed by western blotting with a rat monoclonal anti-HA antibody (clone 3F10).

MTT assay

In this assay, viable cells convert the soluble dye MTT to insoluble blue formazan crystals. NHNP cells were seeded on 48-well flat-bottomed microplates coated with polyethyleneimine 24 h before treatment. Cells were infected with Ad-p53, Ad-p53RDL1 or Ad-LacZ and incubated with 200 ng ml^{-1} GST–Netrin or GST alone. After 48–72 h incubation, 150 μl of MTT tetrazolium salt solution dissolved in culture medium to a final concentration of 0.5 mg ml^{-1} was added to the cells for 4 h. Formazan crystals were dissolved in 150 μl of lysis buffer (0.04 N HCl in isopropanol) before incubation overnight at 37 °C. Experiments were repeated at least three times. Absorbance of the solubilized formazan was measured at 570 nm using a microplate reader. The absorbance values of the treated cells were normalized against the controls.

Accession numbers

The GenBank/EMBL/DDBJ accession number for human *p53RDL1* is AB096256.

RECEIVED 18 APRIL 2002; REVISED 23 OCTOBER 2002; ACCEPTED 2 DECEMBER 2002; PUBLISHED 24 FEBRUARY 2003.

1. Llambi, F., Causeret, F., Bloch-Gallego, E. & Mehlen, P. Netrin-1 acts as a survival factor via its receptors UNC5H and DCC. *EMBO J.* **20,** 2715–2722 (2001).
2. Greenblatt, M. S., Bennett, W. P., Hollstein, M. & Harris, C. C. Mutations in the *p53* tumor suppressor gene: clues to cancer etiology and molecular pathogenesis. *Cancer Res.* **54,** 4855–4878 (1994).
3. Ko, L. J. & Prives, C. p53: puzzle and paradigm. *Genes Dev.* **10,** 1054–1072 (1996).
4. el-Deiry, W. S. *et al.* WAF1, a potential mediator of p53 tumor suppression. *Cell* **75,** 817–825 (1993).
5. Tanaka, H. *et al.* A ribonucleotide reductase gene involved in a p53-dependent cell-cycle check point for DNA damage. *Nature* **404,** 42–49 (2000).
6. Yamaguchi, T. *et al.* p53R2-dependent pathway for DNA synthesis in a p53-regulated cell cycle checkpoint. *Cancer Res.* **61,** 8256–8262 (2001).
7. Miyashita, T. & Reed, J. C. Tumor suppressor p53 is a direct transcriptional activator of the human *bax* gene. *Cell* **80,** 293–299 (1995).
8. Oda, E. *et al.* Noxa, a BH3-only member of the bcl-2 family and candidate mediator of p53-induced apoptosis. *Science* **288,** 1053–1058 (2000).
9. Oda, K. *et al.* p53AIP1, a potential mediator of p53-dependent apoptosis, and its regulation by Ser-46-phosphorylated p53. *Cell* **102,** 849–862 (2000).
10. Matsuda, K. *et al.* p53AIP1 regulates the mitochondrial apoptotic pathway. *Cancer Res.* **62,** 2883–2889 (2002).
11. Owen-Schaub, L. B. *et al.* Wild-type human p53 and a temperature-sensitive mutant induce Fas/APO-1 expression. *Mol. Cell Biol.* **15,** 3032–3040 (1995).
12. Wu, G. S. *et al.* KILLER/DR5 is a DNA damage-inducible p53-regulated death receptor gene. *Nature Genet.* **17,** 141–143 (1997).
13. Okamura, S. *et al. p53DINP1*, a p53-inducible gene, regulates p53-dependent apoptosis. *Mol. Cell* **8,** 85–94 (2001).
14. Tokino, T. *et al.* p53-tagged sites from human genomic DNA. *Hum. Mol. Genet.* **3,** 1537–1542 (1994).
15. Ono, K. *et al.* Identification by cDNA microarray of genes involved in ovarian carcinogenesis. *Cancer Res.* **60,** 5007–5011 (2000).
16. El-Deiry, W. S., Kern, S. E., Pietenpol, J. A., Kinzler, K. W. & Vogelstein, B. Definition of a consensus binding site for p53. *Nature Genet.* **1,** 45–49 (1992).
17. Tessier-Lavigne, M. & Goodman, C. S. The molecular biology of axon guidance. *Science* **247,** 1123–1133 (1996).
18. Serafini, T. *et al.* Netrin-1 is required for commissural axon guidance in the developing vertebrate nervous system. *Cell* **87,** 1001–1014 (1996).
19. Colamarino, S. A. & Tessier-Lavigne, M. The axonal chemoattractant netrin-1 is also a chemorepellent for trochlear motor axons. *Cell* **81,** 621–629 (1995).
20. Mehlen, P. *et al.* The *DCC* gene product induces apoptosis by a mechanism requiring receptor proteolysis. *Nature* **395,** 801–804 (1998).
21. Forcet, C. *et al.* The dependence receptor DCC (deleted in colorectal cancer) defines an alternative mechanism for caspase activation. *Proc. Natl Acad. Sci. USA* **98,** 3416–3421 (2001).

Acknowledgements
We thank B. Vogelstein for the *p53*-deficient cancer cell lines, and P. Mehlen for the recombinant netrin protein. We also thank K. Matsui and S. Onoue for their excellent technical assistance. This work was supported in part by Grants #13216031 & #14028018 from the Ministry of Education, Culture, Sports, Science and Technology (to H.A.), in part by Research Grant #01-23301 of the Princess Takamatsu Cancer Research Fund (to H.A.) and in part by "Research for the Future" Program Grant #00L01402 from the Japan Society for the Promotion of Science (to Y.N.).
Correspondence and requests for material should be addressed to H.A.

COMPETING FINANCIAL INTERESTS
The authors declare that they have no competing financial interests.